Research Article

Przemyslaw Lopato*

Pulsed excitation terahertz tomography – multiparametric approach

https://doi.org/10.1515/phys-2018-0018
Received Nov 02, 2017; accepted Nov 12, 2017

Abstract: This article deals with pulsed excitation terahertz computed tomography (THz CT). Opposite to x-ray CT, where just a single value (pixel) is obtained, in case of pulsed THz CT the time signal is acquired for each position. Recorded waveform can be parametrized - many features carrying various information about examined structure can be calculated. Based on this, multiparametric reconstruction algorithm was proposed: inverse Radon transform based reconstruction is applied for each parameter and then fusion of results is utilized. Performance of the proposed imaging scheme was experimentally verified using dielectric phantoms.

Keywords: electromagnetic waves, terahertz imaging, tomography, reconstruction, artificial neural networks

PACS: 81.70.Tx, 84.40.-x, 81.70.Ex

1 Introduction

Electromagnetic waves in terahertz frequency range (T-rays) enable non-invasive, non-contact and non-ionizing inspection of dielectric materials and semiconductors. T-rays are sensitive to complex permittivity changes, therefore any defect or structure detail causing its noticeable disturbance can be detected. The most common method of defects localization is transmission or reflection imaging based on pulsed terahertz Time Domain Spectroscopy (THz TDS) [1–5].

Tomography is defined as the cross-sectional imaging of an object under test (OUT) by measuring scattered wave (rays). There are several terahertz imaging techniques [6–10]:

- time of flight reflection tomography (THz ToFRT),
- digital holography,
- diffraction tomography (THz DT),
- tomography with binary lens,
- computed tomography (THz CT).

Terahertz CT enables analogous to conventional x-ray CT reconstruction of the objects physical properties distribution based on sectional slices (Figure 1). However, in case of terahertz tomography both amplitude and phase data are collected (opposite to intensity of radiation for x-ray CT). The above fact causes that THz CT provides more information about the examined object [1]. For each slice object under test is rotated by angle Θ and shifted by distance r. The terahertz radiation passing through the object is recorded in the measuring plane, where the projection $R(\Theta, r)$ is obtained. In Ref. [7] it has been shown that the change in phase of the electromagnetic wave in the measuring plane can be used to determine the distribution of the refractive index n (and consequently permittivity ϵ) in the cross-section of the object. Forward problem (projection $R(\Theta, r)$ calculation) mathematically is described by Radon transform [7, 9, 11]:

$$R(\Theta, r) = \int_{-\infty}^{\infty}\int_{-\infty}^{\infty} g(x, y)\ \delta(r - x\cos\Theta - y\sin\Theta)\ dxdy \quad (1)$$

where: $g(x,y)$ – spatial distribution of the selected electromagnetic parameter of the imaged object, e.g. refractive index $n(x, y)$, $\delta(\bullet)$ – Dirac delta function, Θ – projection angle, r – ray distance from the axis of rotation.

The inverse problem – the reconstruction of the spatial distribution of the OUT's electromagnetic parameters – is mathematically described by the inverse Radon transform [9, 11]:

$$g_R(x, y) = \int_{0}^{\pi}\int_{-\infty}^{\infty} R(\Theta, r)\ \delta(r - x\cos\Theta - y\sin\Theta)\ drd\Theta \quad (2)$$

In this paper terahertz computed tomography system with pulsed excitation is shown. Moreover, the reconstruction algorithm based on standard inverse Radon transform (2) and artificial neural network is proposed and verified us-

*Corresponding Author: Przemyslaw Lopato: Department of Theoretical Electrical Engineering and Computer Science, West Pomeranian University of Technology, Szczecin, Poland; Email: plopato@zut.edu.pl

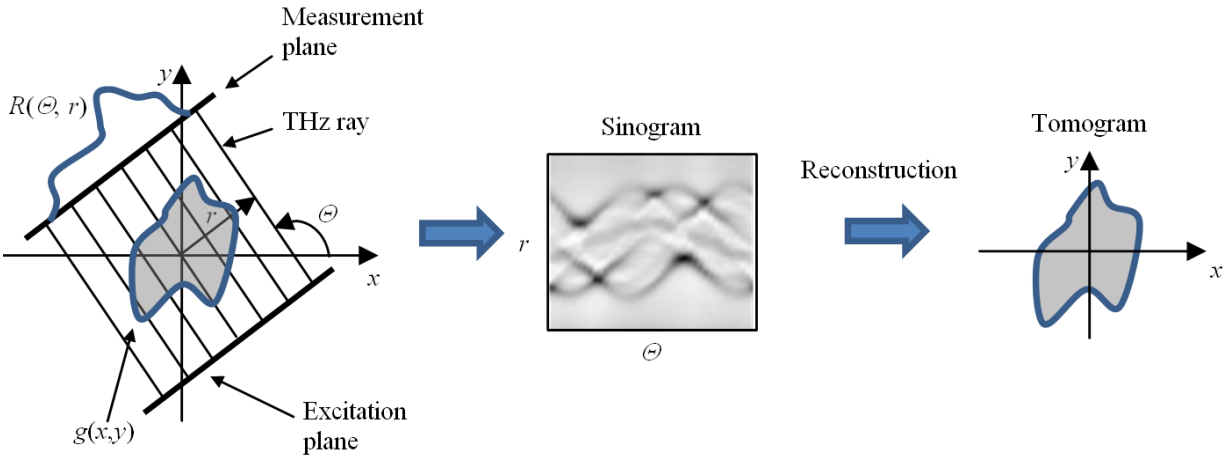

Figure 1: Simplified scheme of THz CT principle of operation

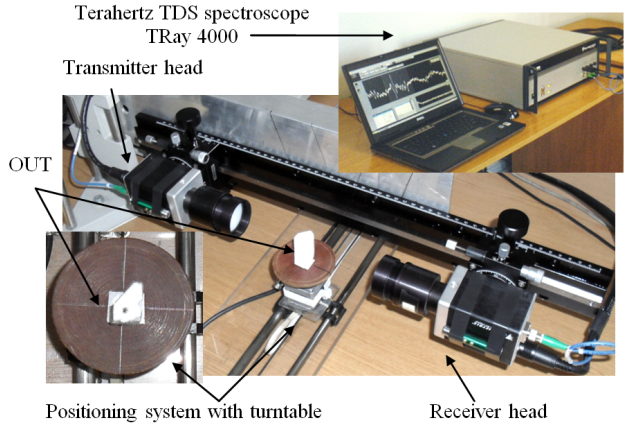

Figure 2: Photo of utilized pulsed THz CT system

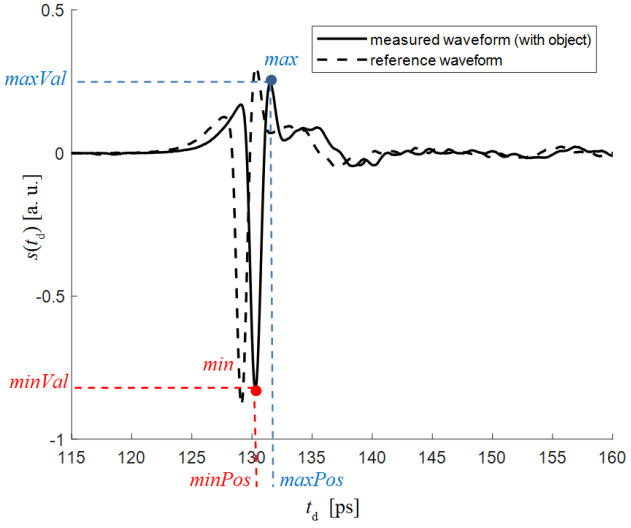

Figure 3: Measured signal $s(t)$ obtained for each position and definitions of basic parameters in the time domain (*maxVal*, *maxPos*, *minVal* and *minPos*)

ing tomographic inspections of phantoms made of foamed polystyrene.

2 Measuring system

The proposed tomographic system is based on TRay4000 pulsed terahertz spectroscope of Picometrix (Figure 2). Picosecond order pulses are generated and detected by transmitter and receiver heads using photoconductive antennas (PCA). Terahertz beam focused by HDPE lenses is transmitted through examined object. The OUT was mounted on a (Θ, r, z) rotation/translation stage and scanned in order to obtain a slice image. For each position r and projection angle Θ, a transmission measurement is performed and a time-domain signal $s(t)$ is recorded. Exemplary waveform obtained during tomographic inspection as well as some basic features of THz pulse are shown in Figure 3. Whole system was controlled by a software implemented in Matlab environment.

3 Reconstruction algorithm

Other (than phase shift) parameters of the signal measured in the measurement plane may be used for reconstruction. In the case of pulsed excitation (TDS), the pulse energy, amplitude or time delay introduced by the presence of the object is determined. Time signal acquisition makes it possible to design a very large number of time domain (TD), frequency (FD) and joint time-frequency domain (TFD) parameters. Depending on the parameter used during reconstruction, the resulting image (slice) will have

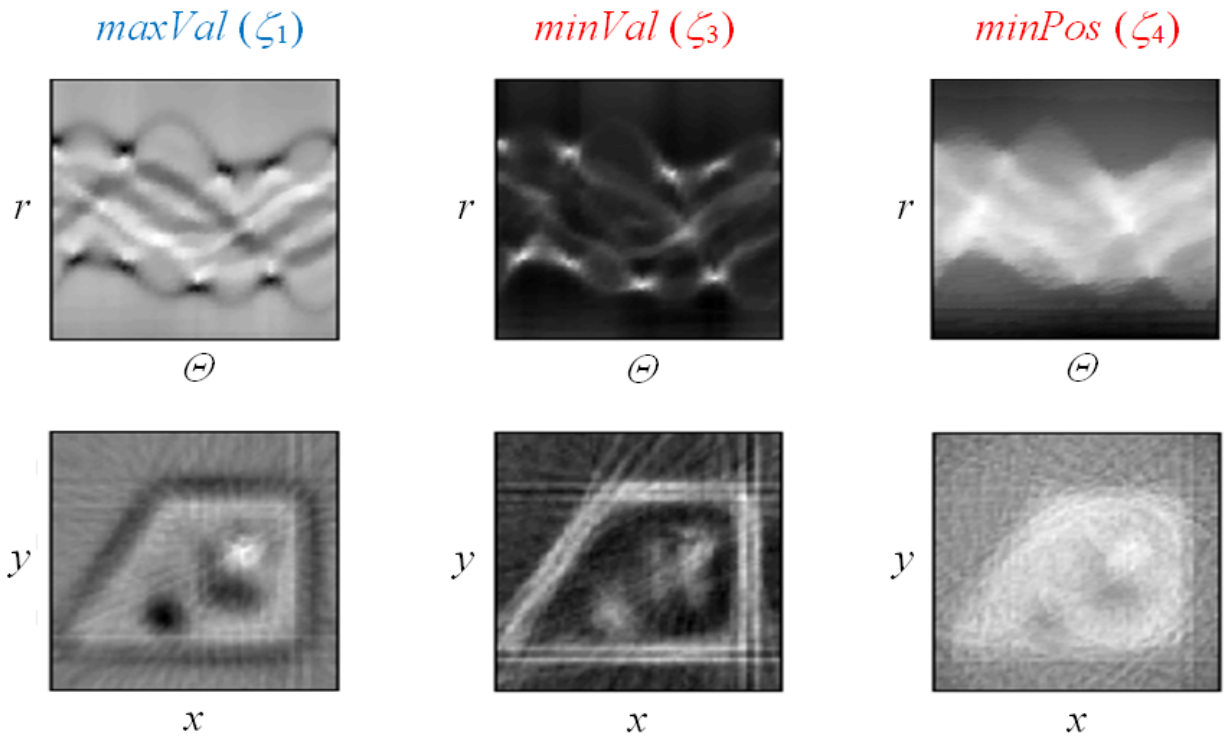

Figure 4: Sinograms (up) and results of the reconstruction (down) of the object containing the defect for various parameters used in the reconstruction process (*maxVal*, *minVal* and *minPos*)

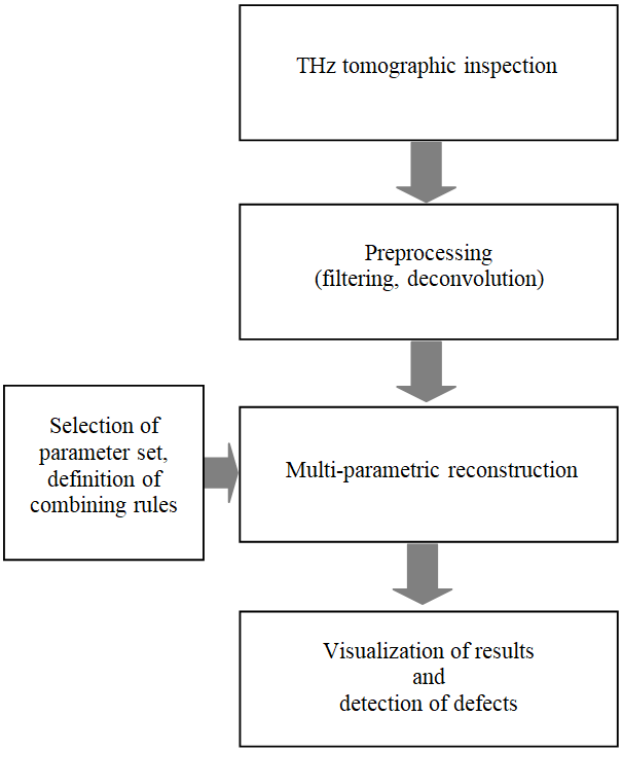

Figure 5: Scheme of multiple parameters reconstruction algorithm

a different character, *i.e.* other features will be exposed. For example, the use of frequency parameters (the amplitudes of different harmonics) will increase the sensitivity of detection of materials with different frequency dependent refractive indices or absorption coefficients. The use of multiple parameters reconstruction and subsequent fusion of the resulting distributions enables to achieve better results, which will be shown later in this paper. Generally, the multiparametric approach is becoming more popular in non-destructive testing [12].

Based on acquired $s(t)$ time-domain waveform, a set of features ζ_n was calculated both in time and frequency domain. Each obtained parameter ζ_n can be utilized in order to form a sinogram (Figure 1). Sinograms acquired by measurements as well as reconstruction results using inverse Radon transform [11] in case of selected parameters ζ_n of waveform $s(t)$ are shown in Figure 4. Based on observable differences in obtained images, the following conclusion can be drawn – selected parameters carry various information content about spatial distribution of dielectric properties in object under test. Therefore, multiparametric reconstruction algorithm using Radon's inverse transformation and artificial neural networks in the process of combining information derived from different parameters is proposed. The block diagram of the proposed procedure is shown in Figure 5. The first step is to perform an inspec-

Table 1: Parameters utilized for reconstruction

No.	Parameters	
	Definition	***Description***
1.	$\zeta_1 = \max[s(t)] = maxVal$	maximum value of $s(t)$ signal (*maxVal* in Figure 3)
2.	$\zeta_2 = t_{d\max}$	time delay at which the maximum value of the signal occurs (*maxPos* in Figure 3)
3.	$\zeta_3 = \min[s(t)] = \min Val$	minimum value of $s(t)$ signal (*minVal* in Figure 3)
4.	$\zeta_4 = t_{d\min}$	time delay at which the minimum value of the signal occurs (*minPos* in Figure 3)
5.	$\zeta_5 = \max[s(t)] - \min[s(t)]$	signal peak-to-peak value
6.	$\zeta_6 = \int_{t_1}^{t_2} \lvert s(t)\rvert\, dt$	area under absolute value of signal in time domain
7.	$\zeta_7 = mean[s(t)]$	mean value of the signal
8.	$\zeta_8 = med[s(t)]$	median of sampled signal
9.	$\zeta_9 = std\ [s(t)]$	standard deviation of the sampled signal
10.	$\zeta_{10} = 10\log_{10}\lvert S(f_1)\rvert$	amplitude of selected harmonic f_1 = 70GHz
11.	$\zeta_{11} = 10\log_{10}\lvert S(f_3)\rvert$	amplitude of selected harmonic f_2 = 250GHz
12.	$\zeta_{12} = 10\log_{10}\lvert S(f_5)\rvert$	amplitude of selected harmonic f_3 = 1.3THz

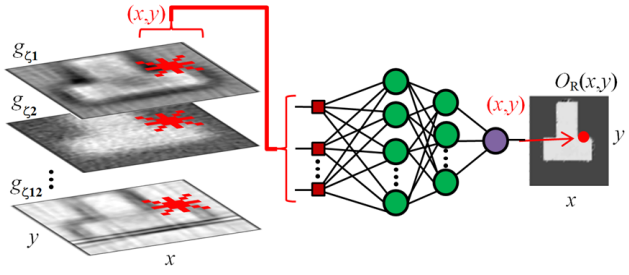

Figure 6: Scheme of multiple parameters fusion using artificial neural network; $g_{\zeta n}(x,y)$ – reconstruction result based on inverse Radon transform and ζ_n parameter of waveform $s(t)$

tion using the developed tomographic system. Then a preprocessing in form of filtration and deconvolution is carried out. Filtration may be implemented in the form of a one-dimensional median filter applied directly to the measurement signal $s(t)$ or a two-dimensional median filter applied on the sinogram $R_M(\Theta, r)$. In both cases, instead of median filtration, one- or two-dimensional wavelet denoising may be used. Another task implemented at this stage is the deconvolution of the sinogram $R_M(\Theta, r)$ – blur limiting operation due to utilization of terahertz Gaussian beam instead of the straight ray beam. The data processed in this way are used in the next step – multi-parametric reconstruction. It is schematically presented in Figure 6.

Twelve two-dimensional distributions of selected parameters $\zeta_n(x,y)$ - obtained by reconstruction using the inverse Radon transform - were scanned by the sliding window as shown in Figure 6. A set of 12 parameters from 27 initial ones was selected based on a preliminary analysis of the signal to noise ratio (SNR). Their definitions are presented in Table 1. Both time domain features ($\zeta_1 - \zeta_9$) and frequency domain ($\zeta_{10} - \zeta_{12}$) were used. Reconstructions obtained using the selected parameters enable identification of both the edges of the examined phantoms and the objects inside the structure, such as artificial or real defects. They contain a variety of information about the OUT. Data from the window that moves over 12 concurrent reconstructions (based on 12 different parameters) is given to the input of a previously trained artificial neural network (ANN). The neural model estimates the value of the final reconstruction O_R for the position determined by the center of the sliding window (x, y). Three-layer network was used: 2 hidden layers with sigmoidal activation function and 1 output layer with linear activation function. The neural network was trained using the Levenberg-Marquardt method.

4 Results

In order to determine the parameters of proposed reconstruction procedure and neural model, the following criterion of reconstructed image evaluation was proposed:

$$K_R(w_{ms}, N_A, k_\zeta) = K_{FN}(w_{ms}, N_A, k_\zeta) \cdot K_{FP}(w_{ms}, N_A, k_\zeta) \quad (3)$$

where: K_R – criterion for evaluation of the reconstruction result by the proposed procedure, w_{ms} – size of the sliding window, N_A – number of neurons in the neural model, k_ζ – number of ζ_n parameters used for reconstruction, K_{FN} – sum of false negative indications, K_{FP} – sum of false positive indications.

Such simple criterion can be utilized because of quasi-homogenous character of utilized phantoms. For all considered criteria (K_{FN}, K_{FP} and K_R), the smaller the value, the better is the result of the reconstruction. Thus, the minimum value of K_R will be sought to determine the parameters of the utilized neural model. In further analysis, the above criterion will be used in a standardized form:

$$K_{RN} = \frac{K_R}{\max(K_R)} \tag{4}$$

An experiment was conducted, in which the influence of the number of parameters used in the reconstruction on its quality was investigated. The size of sliding window ranged from 3 to 11 and total number of neurons in ANN ranged from 10 to 60. For each combination of (w_{ms}, N_A, k_ζ), 100 networks were trained based on T-shape phantom presented in Figure 7. The validation was performed using several phantoms of different shape. Exemplary results of reconstruction using standard inverse Radon transform and proposed procedure are presented in Figure 8. In case of proposed method, one can observe blur reduction and better defined phantom edges (no oscillation at the air-phantom boundary), compared to standard procedure. This allows a more accurate determination of the size of the examined object and its details. The disadvantage of the proposed algorithm is the need to train a neural model for combining data from various parameters. An influence of number of parameters on reconstruction quality is shown in Figure 9. The order of the features used in this experiment was chosen randomly. One can observe, the reconstruction error (K_{RN}) decreases nonlinearly with increase of k_ζ. Utilization of 4 parameters causes noticeably smaller K_{RN} than in case of one parameter. Further increase of k_ζ doesn't affect the reconstruction error noticeably.

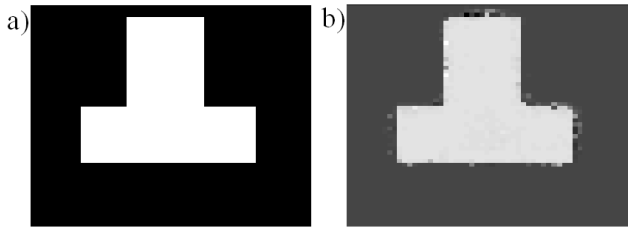

Figure 7: The training set defined by the cross-sectional photo of T-shape phantom (a) and the response of the trained neural model for the training set (b)

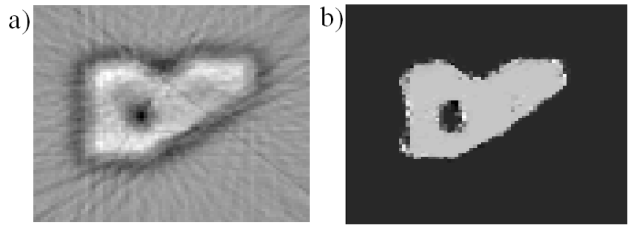

Figure 8: Exemplary reconstruction results for the phantom with artificial defect: a) using inverse Radon transform based on 1 parameter (signal peak-to-peak value), b) using multi-parametric reconstruction

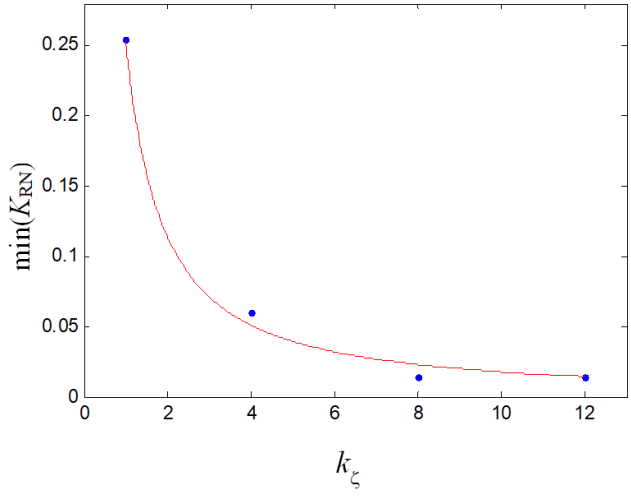

Figure 9: Criterion for evaluation a trained neural model related to the number of parameters used for training

5 Conclusions

The proposed THz CT system and multiparametric algorithm enable proper reconstruction of the considered objects cross-section (as shown in Figure 8) and cause blur reduction of the resulting image. Moreover, the algorithm enables reduction of reconstruction error in comparison to the case of single parameter based inversion (as shown in Figure 9). That proves correctness of proposed multiparametric approach.

The drawback of proposed algorithm is a necessity of training the neural model, thus it is not as widely applicable as transforms based inversions.

References

[1] Mittelman D., Sensing with terahertz radiation, Springer, Berlin, 2010

[2] Palka N., Miedzińska D., Detailed non-destructive evaluation of UHMWPE composites in the terahertz range, Optical and Quantum Electronics, 2014, 46, 515-525.

[3] Yakovlev E., Zaytsev K., Dolganova I., Yurchenko S., Nondestructive evaluation of polymer composite materials at the manufacturing stage using terahertz pulsed spectroscopy, IEEE Trans. Terahertz Sci. Technol., 2015, 5, 5, 810-816.

[4] Ahi K., Anwar M., Advanced terahertz techniques for quality control and counterfeit detection, Proc. SPIE 9856, Terahertz Physics, Devices, and Systems X: Advanced Applications in Industry and Defense, 98560G, 2016, doi:10.1117/12.2228684

[5] Lopato P., Automatic defect recognition for pulsed terahertz inspection of basalt fiber reinforced composites, Compel, 2016, 35, 4, 1346-1359.

[6] Ferguson B., Wang S., Gray D., Abbott D., Zhang X.C., Towards functional 3D T-ray imaging, Physics in Medicine and Biology, 2002, 47, 3735-3742.

[7] Wang S., Zhang X.C., Pulsed terahertz tomography, Journal of Physics D: Applied Physics, 2004, 37, R1-R36.

[8] Zimdars D., Fichter G., Chemovski A., Time domain terahertz computed axial tomography for nondestructive evaluation, Review of Quantitative Nondestructive Evaluation, 2009, 28, 426-433.

[9] Choi H., Son J.-H., Terahertz imaging and tomography techniques, Terahertz Biomedical Science and Technology, Joo-Hiuk Son (ed.), CRC Press, 2014, 47-66.

[10] Guillet J.P., Recur B., Frederique L., Bousquet B., Canioni L., Manek-Honninger I., Desbarats P., Mounaix P., Review of terahertz tomography techniques, Journal of Infrared, Millimeter and Terahertz Waves, 2014, 35, 382-411.

[11] Kak A.C., Slaney M., Principles of computerized tomographic imaging, IEEE Press, New York, 1988

[12] Psuj G., Fusion of multiple parameters of signals obtained by vector magnetic flux observation for evaluation of stress loaded steel samples, International Journal of Applied Electromagnetics and Mechanics, 2015, 49, 1, 1-7.